Correction of the dispersion in the GERB's detector spectral response curves

Nicolas Clerbaux

July 12, 2007

Ref : MSG-RMIB-GE-TN-0031

Version 2.0

Abstract

This technical note quantifies the errors introduced in the GERB final products due to the dispersion of spectral response (SR) curves between the different GERB detectors. This dispersion is the cause of a dispersion of the detector's filtered radiances for a given observed scene $L(\lambda)$. According to the magnitude of this dispersion, it can be more or less correct to interpolate spatially in a GERB filtered radiance image (level 1.5 data, also called NANRG), as each line is taken by a different detector.

This document proposes a practical way to reduce the problem introduced by this dispersion for the RMIB GERB processing by a preliminary correction of the detector's radiances before the unfiltering process. The proposed correction removes a large part of the dispersion error.

This work is based on the Edition-1 spectral characterization of the GERB-2 instrument. This characterization exhibits only very limited pixel-by-pixel variability because the 256 detectors are supposed to have the same spectral sensitivity. So, the variations of SR are only due to the optical components of the instrument (quartz filter and mirrors) New version of this technical note will be issued when accurate detector level characterization will be available.

Contents

1 Introduction and Spectral Response

1.1 Available spectral response information

At this time, the more realistic characterization of the spectral response of the different GERB-2 pixels (i.e. detector + optical components) is obtained by assuming that the 256 detectors have all the same spectral sensitivity. The detector spectral characterizations appear indeed too noisy to be used without averaging. The pixel level dispersion is then very limited because introduced only by the optical components (quartz filter and mirrors).

A new version of this technical note will be issued when accurate detector level characterization will be available.

1.2 Definition of the GERB averaged SR

The average spectral response curves of the instrument is defined by averaging the detector's spectral response curves

$$\phi_{SW}^{gerb}(\lambda) = \frac{1}{256}\sum_{k=1}^{256}\phi_{SW}^{k}(\lambda) \quad (1)$$

$$\phi_{TOT}^{gerb}(\lambda) = \frac{1}{256}\sum_{k=1}^{256}\phi_{TOT}^{k}(\lambda) \quad (2)$$

$$\phi_{LW}^{gerb}(\lambda) = \frac{1}{256}\sum_{k=1}^{256}\phi_{LW}^{k}(\lambda) \quad (3)$$

Figure (1) shows these curves for the GERB-2 (Edition-1) and GERB-1 (prerelease) instruments.

1.3 Problem statement

Each line in a GERB shortwave (SW) or total (TOT) image corresponds to a different filtered radiance and, strictly speaking, it is not correct to interpolate spatially in these images. In the RMIB GERB Processing (RGP) each line is supposed to be taken by a same detector which has the average spectral response curves defined by Eq.(3). So, it is necessary to convert the detector's radiances into GERB radiances (the radiance that would have been measured by an instrument having the average spectral response curves). This conversion allows the interpolatation within the image because, after conversion, each line corresponds to a same physical quantity.

1.4 Databases of spectral radiance curves $L(\lambda)$

To assess the effect of the SW and LW channel dispersions, 2 databases of simulated spectrums $L(\lambda)$ have been used. These databases are described in (Clerbaux, 2007). The study of the

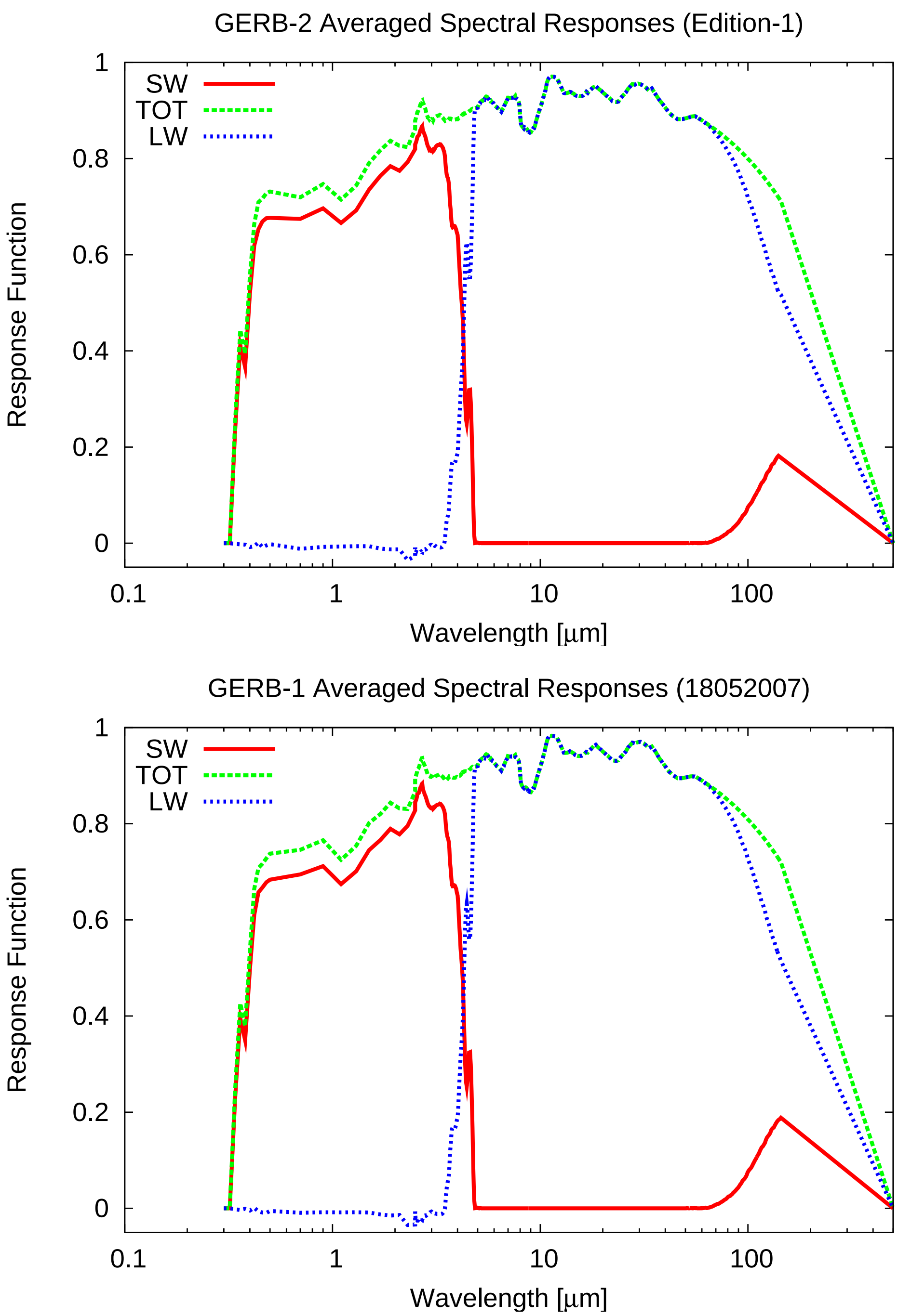

Figure 1: Average spectral response curves for the GERB-2 Edition-1 (top) and GERB-1 prerelease (bottom) instruments.

	unit	ocean	sand (sandst6f)	vegetation (conifers)	snow (medium)	water cloud	ice cloud
min	$Wm^{-2}sr^{-1}$	8.46	75.02	38.95	123.15	151.37	134.73
max	$Wm^{-2}sr^{-1}$	8.48	75.06	38.97	123.25	151.48	134.83
mean	$Wm^{-2}sr^{-1}$	8.47	75.03	38.96	123.18	151.40	134.76
max-min	$Wm^{-2}sr^{-1}$	0.01	0.04	0.02	0.09	0.11	0.10
$\frac{max-min}{mean}$	(%)	0.15	0.06	0.05	0.08	0.07	0.07
std. dev. σ	$Wm^{-2}sr^{-1}$	0.00	0.01	0.01	0.03	0.03	0.03
$\frac{\sigma}{mean}$	(%)	0.04	0.02	0.02	0.02	0.02	0.02

Table 1: Shortwave radiance dispersion for typical scene types. The table is for the GERB-2 spectral response used for the Edition-1.

SW channel dispersion is based on a database of reflected solar radiation $L_{sol}(\lambda)$ while for the LW channel a database of emitted thermal radiation $L_{th}(\lambda)$ is used.

For the SW analysis, an additional database of typical spectrums is used. This database contains SBDART (Ricchiazzi et al., 1998) simulations for ocean, sand, vegetation, snow, water cloud, and ice cloud. The generation of these typical spectrums is also described in (Clerbaux, 2007).

1.5 Simulated filtered radiances

For each simulated spectrum $L_{sol}(\lambda)$ of reflected solar radiation the SW filtered radiances are computed for the 256 detectors and for the average detector

$$L_{SW}^{k} = \int_{0.25}^{5} L_{sol}(\lambda)\phi_{SW}^{k}(\lambda)d\lambda \quad (4)$$

$$L_{SW}^{gerb} = \int_{0.25}^{5} L_{sol}(\lambda)\phi_{SW}^{gerb}(\lambda)d\lambda \quad (5)$$

The LW filtered radiances are computed from the simulated emitted thermal radiation $L_{th}(\lambda)$

$$L_{LW}^{k} = \int_{2.5}^{500} L_{th}(\lambda)\phi_{SW}^{k}(\lambda)d\lambda \quad (6)$$

$$L_{LW}^{gerb} = \int_{2.5}^{500} L_{th}(\lambda)\phi_{SW}^{gerb}(\lambda)d\lambda \quad (7)$$

2 Filtered radiances dispersion

2.1 Shortwave channel dispersion

Table (1) gives, for 6 typical scenes $L(\lambda)$, the minimum, maximum and standard deviation of the distribution of the detector's SW radiance L_{sw}^{k} for the GERB-2 instrument (ED01). With this version of the spectral response curves, the dispersion is quite limited in the SW filtered radiance. The value $(max - min)/mean$ remains under 0.15%.

For 1000 scenes taken randomly in the SW database, the maximal and minimal detector's radiances are computed:

$$L_{SW}^{max,sc} = \max_k (L_{SW}^{k,sc}) \quad (8)$$

$$L_{SW}^{min,sc} = \min_k (L_{SW}^{k,sc}) \quad (9)$$

The red dots on Figure (2,top) shows the difference $L_{SW}^{max,sc} - L_{SW}^{min,sc}$ versus the GERB shortwave radiance $L_{SW}^{gerb,sc}$ of the scene. The $max - min$ dispersion increases with the radiance but remains under the value of $0.18 W m^{-2} sr^{-1}$, even for the brightest scenes.

2.2 Longwave channel dispersion

Figure (2, bottom) represents the same dispersion but for the longwave radiances. The value of the $max - min$ difference is (much) higher than for the SW channel. Differences $max - min$ in filtered radiance higher than $0.5 W m^{-2} sr^{-1}$ are often observed.

Investigation of the LW dispersion shows that the filtered radiance is linearly dependent on the detector number when averaged over a large number of scenes. The following averaged radiances over our database are obtained

- Northest detector $< L > = 61.99 W m^{-2} sr^{-1}$
- Average detector $< L > = 61.82 W m^{-2} sr^{-1}$
- Southest detector $< L > = 61.65 W m^{-2} sr^{-1}$

A half percent difference exists along the GERB detector's array. If we do not correct for this (and it is the case for the Edition-1) we expect to slightly overestimate the Northern hemisphere longwave fluxes and to slightly underestimate in the Southern hemisphere.

3 Conversion of detector radiance into "GERB" radiance

3.1 Errors introduced by the conversion

Let $\widetilde{L^{gerb}}$ be the estimated gerb filtered radiances obtained by conversion of the radiances measured by the k^{th} detector. The relative residual errors for this detectors is estimated as

$$\epsilon_{sw}^{k} = \frac{\sqrt{\frac{1}{N}\sum_{i=1}^{N}(L_{sw}^{gerb} - \widetilde{L_{sw}^{gerb}})^2}}{\frac{1}{N}\sum_{i=1}^{N} L_{sw}^{gerb}}$$

$$\epsilon_{lw}^{k} = \frac{\sqrt{\frac{1}{N}\sum_{i=1}^{N}(L_{lw}^{gerb} - \widetilde{L_{lw}^{gerb}})^2}}{\frac{1}{N}\sum_{i=1}^{N} L_{lw}^{gerb}} \quad (10)$$

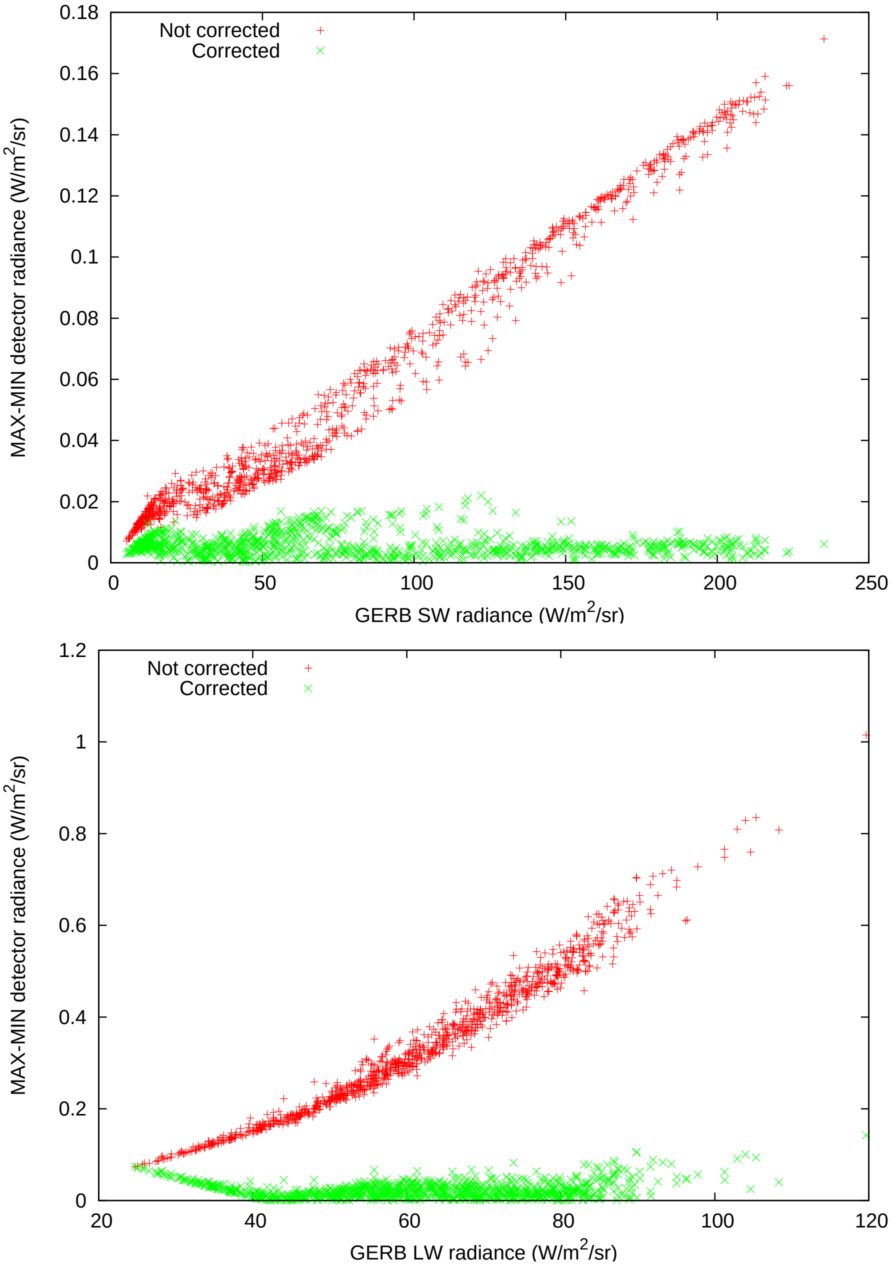

Figure 2: (Max-min) difference of GERB-2 detector's SW (top) and LW (bottom) filtered radiances versus the averaged GERB radiances for 1000 scenes $L(\lambda)$ randomly selected in our databases. The green dots correponds to the dispersion after the linear correction given by Eq.(18).

where the summations are done on the $N = 1000$ spectral radiance curves in the database. The errors (10) are then averaged for all the detectors array (256 detectors):

$$\begin{aligned} \epsilon_{sw} &= \frac{1}{256}\sum_{k=1}^{256} \epsilon_{sw}^k \\ \epsilon_{lw} &= \frac{1}{256}\sum_{k=1}^{256} \epsilon_{lw}^k \end{aligned} \tag{11}$$

3.2 Results supposing $L^k = L^{gerb}$ for all detector

In this case, the filtered GERB radiances are auusmed to be equal to the detector radiances

$$\widetilde{L_{sw}^{gerb}} = L_{sw}^k \tag{12}$$

$$\widetilde{L_{lw}^{gerb}} = L_{lw}^k \tag{13}$$

This assumption is done for the Edition-1 GERB-2 processing. The average residual errors of Eq.(11) gives in this case

$$\epsilon_{sw} = 0.023\% \tag{14}$$

$$\epsilon_{lw} = 0.158\% \tag{15}$$

And the detector with the worse conversion error gives

$$\max_k(\epsilon_{sw}^k) = 0.060\% \tag{16}$$

$$\max_k(\epsilon_{lw}^k) = 0.302\% \tag{17}$$

3.3 Results using first order regression for all detector

In this case, one estimates the filtered GERB radiances as a linear function of the detector radiances:

$$\begin{aligned} \widetilde{L_{sw}^{gerb}} &= a^k + b^k L_{sw}^k \\ \widetilde{L_{lw}^{gerb}} &= c^k + d^k L_{lw}^k \end{aligned} \tag{18}$$

where the regression coefficients $\{a^k, b^k, c^k, d^k)$ for each detector are dependent on its kind of spectral response curves. Using least mean square fitting, one gets (same formula to estimate the long wave coefficients c^k andd^k)

$$b^k = \frac{< L_{sw}^k L_{sw}^{gerb} > - < L_{sw}^k >< L_{sw}^{gerb} >}{< L_{sw}^k L_{sw}^k > - < L_{sw}^k >< L_{sw}^k >} \quad (19)$$

$$a^k = < L_{sw}^{gerb} > -b^k < L_{sw}^k > \quad (20)$$

The values of the best fit parameters a, b, c, d for the 256 detectors of GERB-2 Edition-1 are given in the Table in annexe.

This leads to averaged residual errors (11) of:

$$\epsilon_{sw} = 0.002\% \quad (21)$$

$$\epsilon_{lw} = 0.012\% \quad (22)$$

The detector with the worse conversion error gives

$$\max_k(\epsilon_{sw}^k) = 0.004\% \quad (23)$$

$$\max_k(\epsilon_{lw}^k) = 0.024\% \quad (24)$$

3.4 Comment

The first order regression improves the spectral conversion by a factor of about 10 for the shortwave and longwave channels. When the regressions are used, the maximal error introduced by this spectral conversion is acceptable. This simple conversion does not use any information about the scene spectral signature (the curve $L(\lambda)$) from auxiliary sensor (i.e. SEVIRI). The implementation of this conversion can be done as a separate first step in the GERB/RMIB data processing.

The reduction of the detector's radiance dispersion is illustrated with the green dots on Figures (2). The table hereafter summarizes the values given before.

	Without correction	With correction
mean SW	0.023 %	0.002 %
max SW	0.060 %	0.004 %
mean LW	0.158 %	0.012 %
max LW	0.302 %	0.024 %

4 Possible implementation within the RMIB GERB ground segment

In this section we propose 3 different ways to convert the filtered detector radiance into filtered GERB radiance. In practice the third implementation (see Figure 5) has been adopted for the RGP. The correction has been implemented but is not activated for the Edition-1 GERB-2 processing.

4.1 First implementation

Figure (3) shows a possible implementation of the detector's radiance correction at the beginning of the RMIB GERB processing (RGP). The shortwave detector radiance are first corrected with Eq.(18). It is then possible to perform spatio-temporal interpolation within and between SW images to obtain images of the SW gerb radiance at the geolocation and the timing of each TOT image. An "alternative synthetic longwave" radiance can then be estimated using:

$$L^k_{LW'} = L^k_{TOT} - A^k L^{gerb}_{SW} \tag{25}$$

The alternative LW' detector's radiances can then be corrected. The result of this first part of the processing is a set of two images: the gerb shortwave and longwave radiance. These images are both given at the geolocation and the timing of the GERB total wave channel.

Note that to obtain the same product but at the shortwave geolocation and timing, the correction of the total wave detector's radiances is needed but this is not possible with simple equations like Eq.(18).

4.2 Second implementation

Figure (4) shows a second possible implementation of the correction at the beginning of the RGP. This implementation assumes that the geolocation does not vary strongly between the TOT and SW acquisitions. In this case, the synthetic longwave detector radiance L^k_{LW} can be estimated instead of $L^k_{LW'}$. The process "back to detector radiance" performs the inverse correction

$$L^k_{SW} = \frac{L^{gerb}_{SW} - a^k}{b^k} \tag{26}$$

4.3 Third implementation

Figure (5) shows a third possible implementation of the correction at the beginning of the RGP. This implementation also assumes that the geolocation does not vary strongly between the TOT and SW acquisitions. For this implementation, the detector's radiance correction is done on the LW estimated at the SW geolocation and timing.

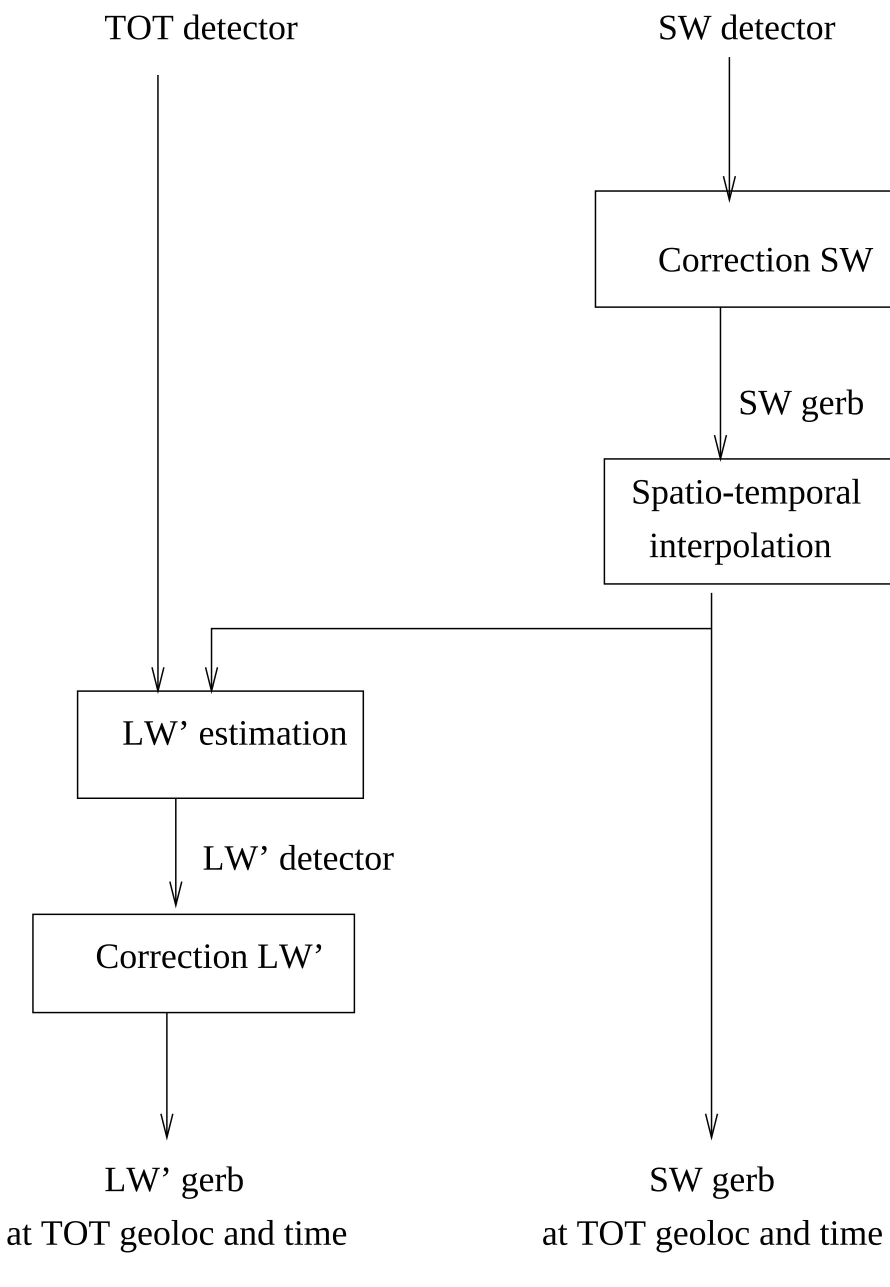

Figure 3: First implementation of the detector's radiances correction at the beginning of the RMIB GERB processing.

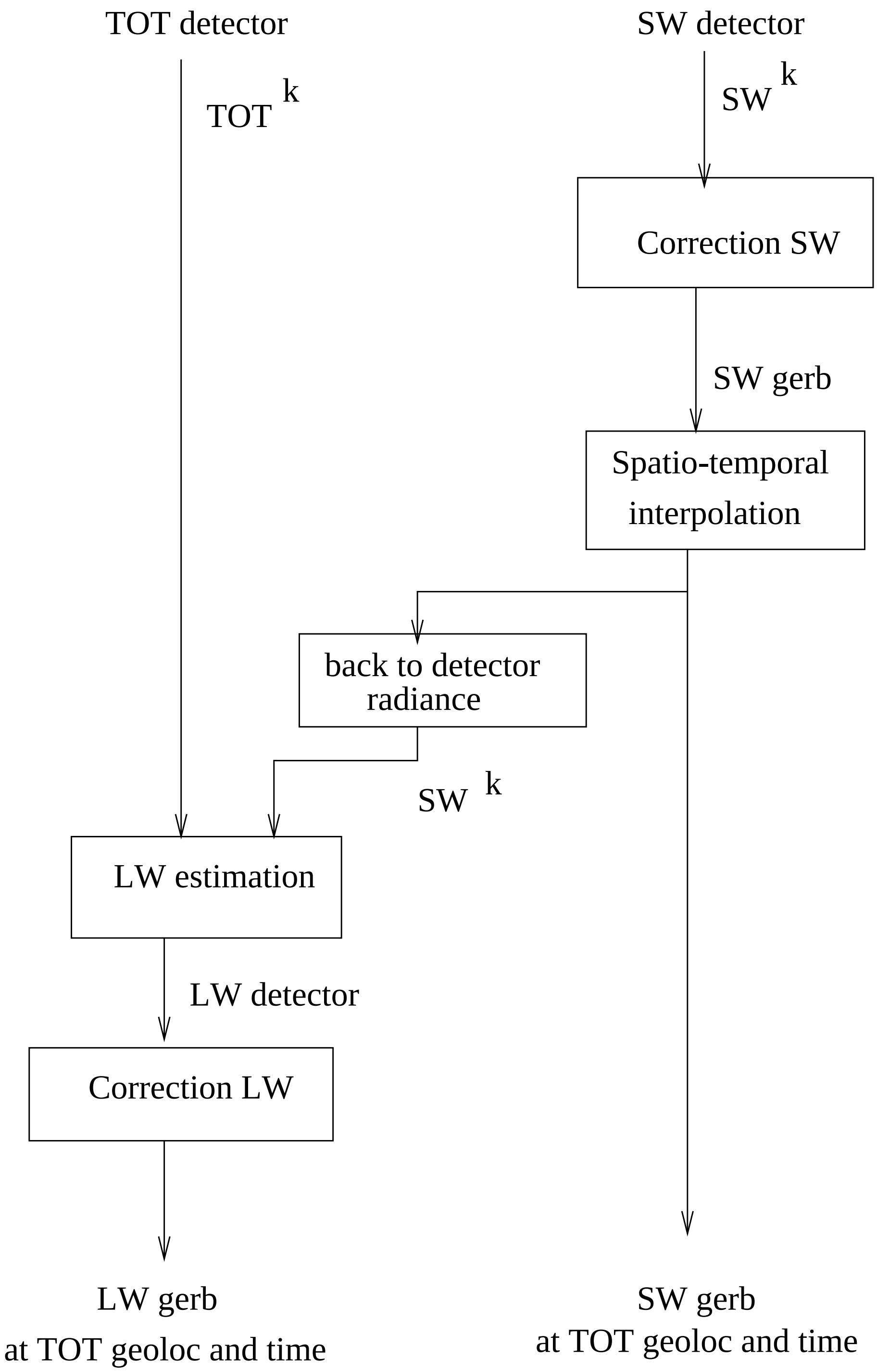

Figure 4: Second implementation of the detector's radiances correction at the beginning of the RMIB GERB processing.

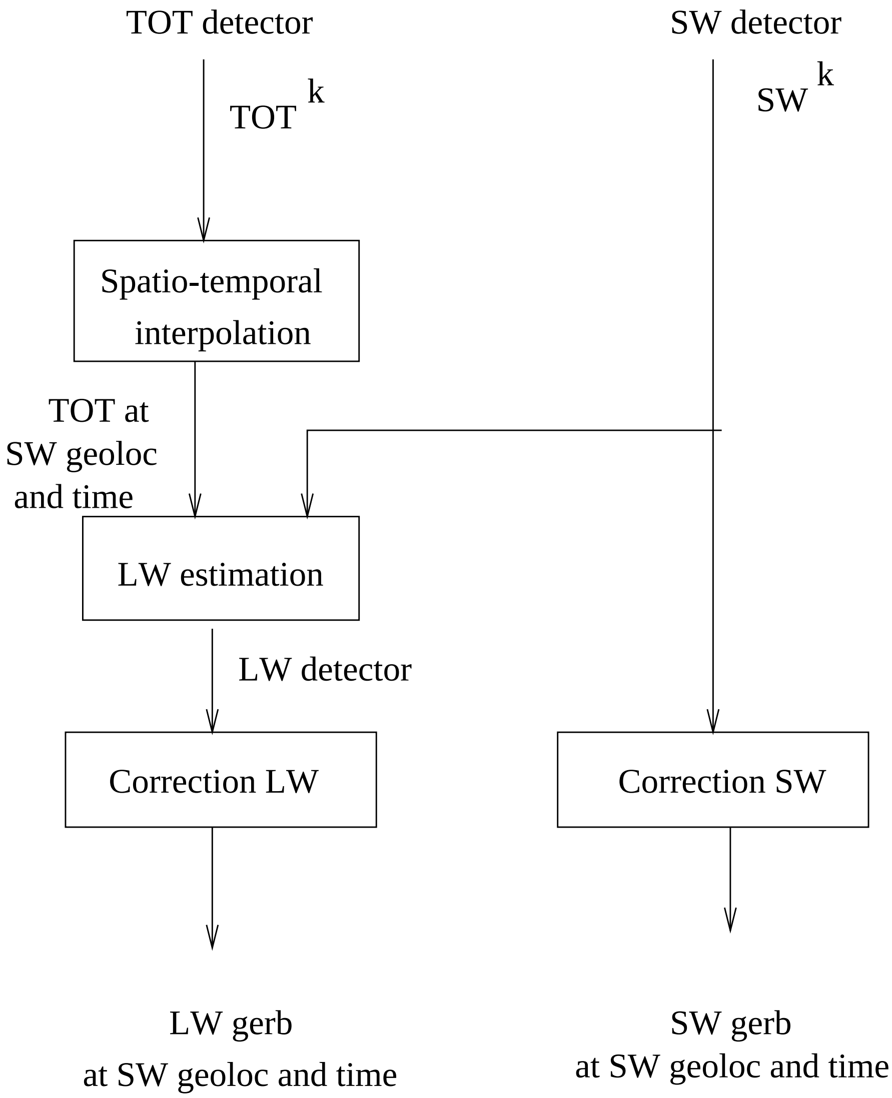

Figure 5: Third implementation of the detector's radiances correction at the beginning of the RMIB GERB processing.

4.4 Comments

The third implementation has been selected for implementation in the RGP because the differences in geolocation between successive TOT and SW acquisitions are small (standard deviation about 0.1 GERB pixel) and because we prefer to do not interpolate spatially in the short wave radiances.

5 Annexe 1: values of the a, b, c, d parameters

k	a^k	b^k	c^k	d^k	k	a^k	b^k	c^k	d^k
1	0	0	0	0	87	-0.000050	0.999931	0.041351	0.998380
2	0	0	0	0	88	-0.000048	0.999933	0.040470	0.998413
3	-0.000132	0.999521	0.108784	0.995483	89	-0.000047	0.999942	0.039587	0.998454
4	-0.000132	0.999538	0.108015	0.995528	90	-0.000042	0.999941	0.038708	0.998485
5	-0.000129	0.999536	0.107239	0.995555	91	-0.000043	0.999943	0.037825	0.998518
6	-0.000128	0.999542	0.106468	0.995590	92	-0.000039	0.999945	0.036944	0.998552
7	-0.000129	0.999541	0.105696	0.995618	93	-0.000033	0.999948	0.036064	0.998587
8	-0.000131	0.999551	0.104926	0.995656	94	-0.000033	0.999952	0.035184	0.998623
9	-0.000130	0.999553	0.104152	0.995687	95	-0.000025	0.999961	0.034301	0.998665
10	-0.000129	0.999557	0.103383	0.995720	96	-0.000029	0.999956	0.033420	0.998690
11	-0.000128	0.999565	0.102609	0.995756	97	-0.000025	0.999965	0.032534	0.998731
12	-0.000130	0.999576	0.101834	0.995796	98	-0.000020	0.999969	0.031658	0.998767
13	-0.000128	0.999579	0.101065	0.995828	99	-0.000019	0.999970	0.030777	0.998800
14	-0.000127	0.999581	0.100289	0.995859	100	-0.000014	0.999975	0.029896	0.998837
15	-0.000129	0.999587	0.099517	0.995893	101	-0.000013	0.999977	0.029014	0.998870
16	-0.000125	0.999593	0.098741	0.995929	102	-0.000012	0.999980	0.028131	0.998905
17	-0.000128	0.999595	0.097972	0.995959	103	-0.000010	0.999985	0.027249	0.998942
18	-0.000125	0.999603	0.097197	0.995995	104	-0.000006	0.999991	0.026364	0.998981
19	-0.000130	0.999608	0.096427	0.996029	105	-0.000005	1.000002	0.025485	0.999022
20	-0.000125	0.999610	0.095653	0.996060	106	0.000001	1.000001	0.024602	0.999053
21	-0.000123	0.999614	0.094881	0.996093	107	0.000001	1.000010	0.023722	0.999094
22	-0.000125	0.999624	0.094104	0.996132	108	0.000003	1.000009	0.022839	0.999125
23	-0.000124	0.999626	0.093334	0.996163	109	0.000008	1.000005	0.021957	0.999153
24	-0.000125	0.999632	0.092558	0.996197	110	0.000012	1.000015	0.021073	0.999195
25	-0.000120	0.999639	0.091787	0.996233	111	0.000015	1.000022	0.020194	0.999234
26	-0.000124	0.999645	0.091013	0.996268	112	0.000018	1.000019	0.019310	0.999262
27	-0.000126	0.999650	0.090240	0.996301	113	0.000021	1.000031	0.018429	0.999307
28	-0.000122	0.999650	0.089466	0.996331	114	0.000021	1.000025	0.017546	0.999332
29	-0.000122	0.999656	0.088693	0.996366	115	0.000024	1.000034	0.016665	0.999373
30	-0.000124	0.999662	0.087920	0.996400	116	0.000027	1.000037	0.015779	0.999408
31	-0.000121	0.999670	0.087149	0.996437	117	0.000030	1.000047	0.014896	0.999449
32	-0.000124	0.999674	0.086373	0.996470	118	0.000035	1.000047	0.014014	0.999482
33	-0.000123	0.999680	0.085596	0.996504	119	0.000037	1.000054	0.013133	0.999520
34	-0.000122	0.999684	0.084829	0.996537	120	0.000040	1.000049	0.012250	0.999548
35	-0.000124	0.999690	0.084054	0.996572	121	0.000039	1.000062	0.011369	0.999592
36	-0.000121	0.999696	0.083277	0.996607	122	0.000044	1.000066	0.010487	0.999628
37	-0.000122	0.999697	0.082503	0.996637	123	0.000047	1.000066	0.009601	0.999660
38	-0.000120	0.999706	0.081730	0.996674	124	0.000047	1.000072	0.008721	0.999697
39	-0.000120	0.999705	0.080956	0.996703	125	0.000055	1.000067	0.007836	0.999725
40	-0.000121	0.999716	0.080181	0.996742	126	0.000054	1.000077	0.006949	0.999767
41	-0.000119	0.999719	0.079408	0.996775	127	0.000058	1.000082	0.006069	0.999804
42	-0.000122	0.999722	0.078634	0.996805	128	0.000056	1.000088	0.005188	0.999841
43	-0.000117	0.999731	0.077860	0.996843	129	0.000055	1.000090	0.004145	0.999883
44	-0.000119	0.999735	0.077082	0.996876	130	0.000051	1.000091	0.003107	0.999924
45	-0.000119	0.999740	0.076314	0.996910	131	0.000047	1.000087	0.002064	0.999959
46	-0.000116	0.999747	0.075536	0.996946	132	0.000044	1.000090	0.001029	1.000002
47	-0.000122	0.999747	0.074766	0.996974	133	0.000042	1.000095	-0.000013	1.000047
48	-0.000116	0.999755	0.073990	0.997012	134	0.000036	1.000099	-0.001055	1.000090
49	-0.000118	0.999760	0.073214	0.997046	135	0.000034	1.000095	-0.002091	1.000127
50	-0.000118	0.999769	0.072439	0.997084	136	0.000033	1.000106	-0.003134	1.000178
51	-0.000117	0.999774	0.071667	0.997117	137	0.000029	1.000104	-0.004175	1.000215
52	-0.000117	0.999777	0.070890	0.997149	138	0.000025	1.000105	-0.005213	1.000256
53	-0.000114	0.999780	0.070118	0.997181	139	0.000023	1.000107	-0.006256	1.000298
54	-0.000116	0.999787	0.069342	0.997217	140	0.000018	1.000114	-0.007296	1.000345
55	-0.000117	0.999787	0.068570	0.997245	141	0.000016	1.000111	-0.008333	1.000382
56	-0.000114	0.999797	0.067795	0.997285	142	0.000012	1.000117	-0.009377	1.000427
57	-0.000113	0.999808	0.067019	0.997324	143	0.000007	1.000119	-0.010415	1.000469
58	-0.000117	0.999810	0.066245	0.997355	144	0.000005	1.000116	-0.011458	1.000506
59	-0.000113	0.999811	0.065471	0.997386	145	0.000003	1.000115	-0.012498	1.000545
60	-0.000116	0.999811	0.064692	0.997414	146	-0.000000	1.000118	-0.013540	1.000588
61	-0.000112	0.999820	0.063921	0.997452	147	-0.000005	1.000120	-0.014582	1.000629
62	-0.000111	0.999829	0.063144	0.997489	148	-0.000009	1.000120	-0.015621	1.000669
63	-0.000115	0.999831	0.062370	0.997520	149	-0.000015	1.000122	-0.016660	1.000711
64	-0.000111	0.999837	0.061595	0.997555	150	-0.000014	1.000127	-0.017705	1.000757
65	-0.000110	0.999840	0.060715	0.997590	151	-0.000018	1.000127	-0.018746	1.000796
66	-0.000109	0.999850	0.059835	0.997631	152	-0.000023	1.000129	-0.019787	1.000837
67	-0.000105	0.999851	0.058956	0.997664	153	-0.000025	1.000131	-0.020829	1.000879
68	-0.000103	0.999853	0.058081	0.997698	154	-0.000028	1.000134	-0.021870	1.000922
69	-0.000097	0.999858	0.057196	0.997735	155	-0.000032	1.000136	-0.022914	1.000965
70	-0.000099	0.999858	0.056315	0.997766	156	-0.000032	1.000135	-0.023955	1.001004
71	-0.000092	0.999868	0.055434	0.997809	157	-0.000040	1.000149	-0.024998	1.001057
72	-0.000094	0.999867	0.054553	0.997839	158	-0.000043	1.000034	-0.026036	1.000982
73	-0.000089	0.999872	0.053675	0.997876	159	-0.000043	1.000144	-0.027080	1.001132
74	-0.000086	0.999874	0.052796	0.997909	160	-0.000047	1.000146	-0.028121	1.001174
75	-0.000085	0.999876	0.051917	0.997943	161	-0.000052	1.000151	-0.029164	1.001218
76	-0.000082	0.999882	0.051035	0.997982	162	-0.000058	1.000148	-0.030208	1.001255
77	-0.000079	0.999885	0.050154	0.998016	163	-0.000059	1.000150	-0.031246	1.001298
78	-0.000076	0.999886	0.049275	0.998049	164	-0.000064	1.000155	-0.032290	1.001341
79	-0.000073	0.999891	0.048395	0.998086	165	-0.000066	1.000151	-0.033332	1.001378
80	-0.000071	0.999900	0.047514	0.998126	166	-0.000070	1.000155	-0.034377	1.001421
81	-0.000066	0.999909	0.046638	0.998167	167	-0.000075	1.000158	-0.035419	1.001465
82	-0.000064	0.999910	0.045757	0.998200	168	-0.000078	1.000157	-0.036458	1.001503
83	-0.000062	0.999913	0.044877	0.998235	169	-0.000080	1.000156	-0.037506	1.001542
84	-0.000060	0.999912	0.043993	0.998265	170	-0.000081	1.000161	-0.038547	1.001587
85	-0.000057	0.999929	0.043112	0.998313	171	-0.000086	1.000167	-0.039593	1.001633
86	-0.000052	0.999923	0.042232	0.998340	172	-0.000092	1.000167	-0.040629	1.001673

k	a^k	b^k	c^k	d^k
173	-0.000095	1.000168	-0.041677	1.001715
174	-0.000097	1.000174	-0.042719	1.001760
175	-0.000099	1.000175	-0.043761	1.001802
176	-0.000103	1.000159	-0.044808	1.001824
177	-0.000111	1.000180	-0.045850	1.001885
178	-0.000112	1.000182	-0.046891	1.001928
179	-0.000112	1.000183	-0.047936	1.001969
180	-0.000118	1.000182	-0.048981	1.002008
181	-0.000120	1.000186	-0.050027	1.002052
182	-0.000128	1.000186	-0.051068	1.002091
183	-0.000129	1.000187	-0.052114	1.002132
184	-0.000130	1.000188	-0.053155	1.002173
185	-0.000132	1.000195	-0.054198	1.002221
186	-0.000139	1.000191	-0.055244	1.002256
187	-0.000147	1.000197	-0.056286	1.002301
188	-0.000149	1.000197	-0.057333	1.002342
189	-0.000153	1.000203	-0.058375	1.002387
190	-0.000154	1.000200	-0.059419	1.002425
191	-0.000159	1.000204	-0.060466	1.002469
192	-0.000164	1.000207	-0.061513	1.002512
193	-0.000152	1.000203	-0.062425	1.002542
194	-0.000140	1.000209	-0.063338	1.002583
195	-0.000129	1.000209	-0.064255	1.002617
196	-0.000113	1.000210	-0.065166	1.002653
197	-0.000105	1.000208	-0.066080	1.002685
198	-0.000093	1.000211	-0.066994	1.002723
199	-0.000082	1.000207	-0.067909	1.002754
200	-0.000068	1.000209	-0.068828	1.002791
201	-0.000063	1.000207	-0.069738	1.002823
202	-0.000049	1.000205	-0.070653	1.002856
203	-0.000037	1.000205	-0.071566	1.002890
204	-0.000023	1.000209	-0.072482	1.002929
205	-0.000015	1.000208	-0.073400	1.002963
206	-0.000006	1.000204	-0.074312	1.002993
207	0.000010	1.000209	-0.075229	1.003033
208	0.000019	1.000204	-0.076142	1.003063
209	0.000032	1.000205	-0.077055	1.003098
210	0.000040	1.000211	-0.077971	1.003139
211	0.000049	1.000210	-0.078890	1.003172
212	0.000065	1.000209	-0.079804	1.003206
213	0.000074	1.000208	-0.080718	1.003240
214	0.000088	1.000209	-0.081635	1.003276
215	0.000093	1.000210	-0.082550	1.003311
216	0.000107	1.000210	-0.083463	1.003346
217	0.000119	1.000204	-0.084376	1.003374
218	0.000130	1.000207	-0.085293	1.003412
219	0.000144	1.000204	-0.086208	1.003444
220	0.000154	1.000207	-0.087127	1.003482
221	0.000165	1.000207	-0.088042	1.003516
222	0.000178	1.000200	-0.088956	1.003543
223	0.000188	1.000199	-0.089872	1.003578
224	0.000198	1.000206	-0.090789	1.003619
225	0.000213	1.000206	-0.091705	1.003654
226	0.000221	1.000207	-0.092620	1.003690
227	0.000235	1.000207	-0.093538	1.003724
228	0.000244	1.000209	-0.094455	1.003761
229	0.000256	1.000211	-0.095371	1.003797
230	0.000267	1.000209	-0.096284	1.003830
231	0.000276	1.000210	-0.097201	1.003865
232	0.000288	1.000214	-0.098116	1.003905
233	0.000299	1.000211	-0.099035	1.003936
234	0.000311	1.000214	-0.099952	1.003973
235	0.000320	1.000212	-0.100865	1.004005
236	0.000334	1.000205	-0.101779	1.004035
237	0.000345	1.000213	-0.102699	1.004076
238	0.000351	1.000211	-0.103616	1.004109
239	0.000368	1.000207	-0.104533	1.004140
240	0.000379	1.000208	-0.105449	1.004176
241	0.000391	1.000202	-0.106368	1.004205
242	0.000402	1.000206	-0.107283	1.004244
243	0.000411	1.000205	-0.108202	1.004277
244	0.000424	1.000204	-0.109115	1.004310
245	0.000435	1.000205	-0.110034	1.004346
246	0.000447	1.000213	-0.110953	1.004389
247	0.000456	1.000216	-0.111869	1.004427
248	0.000470	1.000210	-0.112787	1.004456
249	0.000483	1.000213	-0.113703	1.004494
250	0.000494	1.000215	-0.114620	1.004530
251	0.000505	1.000221	-0.115537	1.004572
252	0.000512	1.000214	-0.116456	1.004598
253	0.000521	1.000215	-0.117371	1.004635
254	0.000536	1.000218	-0.118290	1.004672
255	0	0	0	0
256	0	0	0	0

References

Clerbaux, N., 2007: Generation of a data base of TOA spectral radiance fields. Technical Note MSG-RMIB-GE-TN-0030, RMIB.

Ricchiazzi, P., S. Yang, C. Gautier, and D. Sowle, 1998: SBDART: A research and teaching software tool for plane-parallel radiative transfer in the earth's atmosphere. *Bulletin of the American Meteorological Society*, **79**, 2101–2114, available at http://arm.mrcsb.com/sbdart.